Clear Form

Print Form

RYERSON UNIVERSITY

DEPARTMENT OF AEROSPACE ENGINEERING
FACULTY OF ENGINEERING, ARCHITECTURE AND SCIENCE

Course Code: AER 822

Course Title: Avionics Design Project

Semester: W2013

Instructor: Dr. John Enright

Project

Title: Travel/Pitch Simulation

Section Number: 1

Submission Date: 2/18/2013

Due Date: 2/18/2013

Name	Student Number (XXXX99999)	Signature
Mohamed Helal	XXXX10046	

Show

Show

Show

Show

By signing above you attest that you have contributed to this submission and confirm that all work you have contributed to this submission is your own work. Any suspicion of copying or plagiarism in this work will result in an investigation of Academic Misconduct and may result in a "0" on the work, an "F" in the course, or possibly more severe penalties, as well as a Disciplinary Notice on your academic record under the Student Code of Academic Conduct, which can be found online at: www.ryerson.ca/senate/current/pol60.pdf.

v4.0

Table of Contents

LIST OF FIGURES

NOMENCLATURE

L_a Helicopter body to slip ring
L_w Slip ring to counter weight
L_h Pitch bearing to motor shaft
ε Elevation angle
ρ Pitch angle
λ Travel angle
R_m Motor armature resistance
K_{mt} Motor current-torque constant
J_{pm} Propeller moment of inertia
K_f Motor-prop force-thrust constant
F_w Motor-prop force-speed constant
k_{pt} Motor-prop torque-speed constant
k_b Motor voltage constant
J_t Moment of inertia in the travel axis
J_p Moment of inertia in the pitch axis
D_p Damping in pitch axis
D_t Damping in travel axis
K_p Torsional spring constant in pitch axis

CHAPTER 1: INTRODUCTION

Quanser 3-DOF helicopter is an aerospace plant in Figure (1.1) designed and assembled for the main purpose of position control. The helicopter has three degrees of freedom outputs and only two inputs. The three output degrees of freedom are; first, output rotation of the whole helicopter around its elevation axis; second, output rotation of the helicopter body around its pitch axis; finally, output rotation of the whole helicopter around its travel axis. The free body diagram of the helicopter with its three axes is shown below in Figure (1.2). The two inputs of the helicopter that control all three degrees of freedom are two motor – propeller assemblies. The upward net lift force created by the both motor – propeller assemblies controls the rotation of the helicopter around its elevation axis. However the difference between the net lift forces created by the motor – propeller assemblies controls the rotation of the helicopter body around the pitch axis. The change in pitch angle of the helicopter body is the responsible parameter for controlling the rotation of the helicopter around the travel axis. The helicopter is equipped with three encoders positioned such that they provide the user with three main crucial pieces of information which are the elevation angle, the pitch angle and the travel angle. The encoders could also provide the used with the rate of change of the three angles with time.

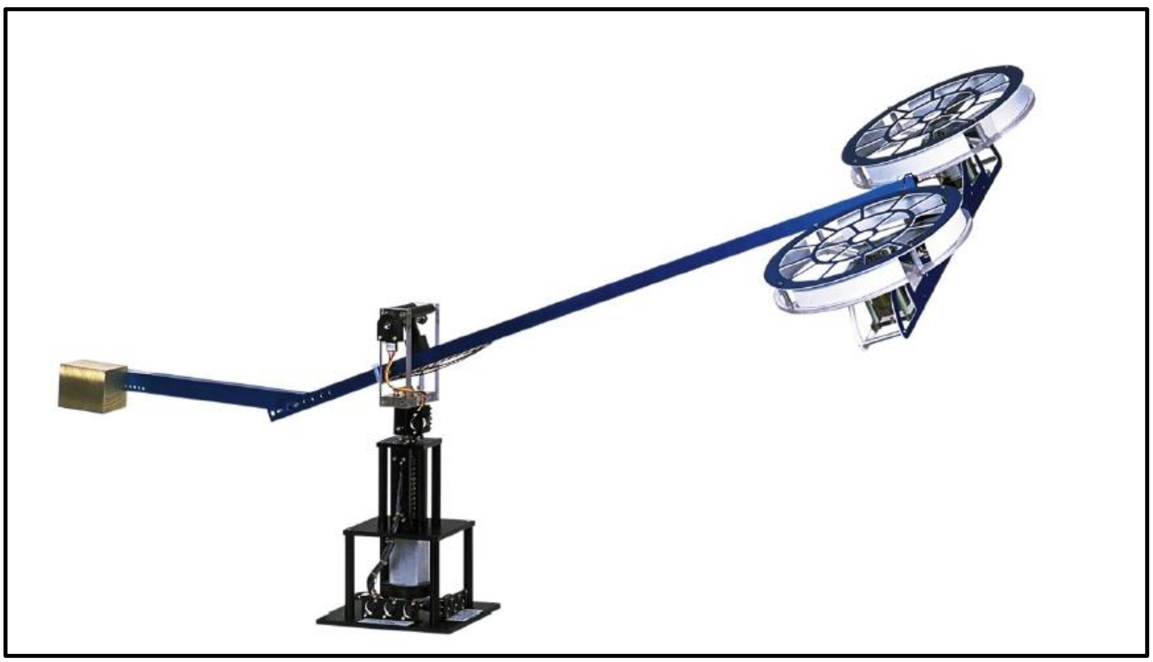

Figure 1.1: Quanser 3-DOF Helicopter [4]

The main objective of this design report is designing a full travel controller that tracks and regulates the rotation of the helicopter around its travel axis. For the purpose of this report the helicopter would be assumed to have a constant leveled elevation angle and the rotation around the elevation axis would not be considered. This report is divided into two main sections that describe the whole process of the design process. The first section is concerned with the modeling of each of the helicopter coupled systems such as the motor – propeller dynamics, the pitch dynamics and the travel dynamics. The second part of this report presents the controller design process based on the derived helicopter models and also includes the method of coupling between the different systems.

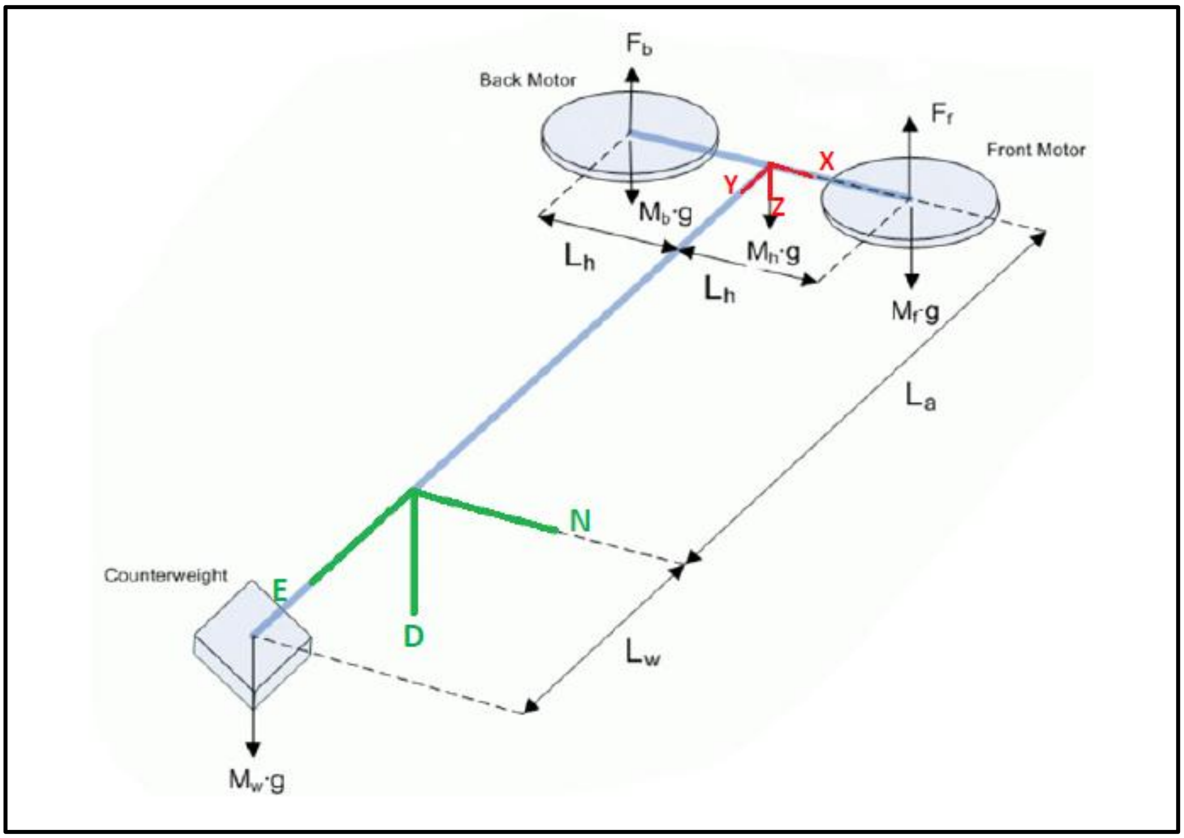

Figure 1.2: Helicopter Free Body diagram [1]

CHAPTER 3: MODELING AND SIMULATION

3.1 Motor – Propeller Dynamics Modeling and Simulation

Mathematical modeling of the dynamics of the motor – propeller assembly units is the first step towards modeling the Quanser helicopter. The Quanser helicopter is equipped with only two motor – propeller assemblies which control all the 3 DOF of the helicopter. The first degree of freedom is the rotation around the elevation axis which is controlled by the upward net amount of the lift force created by the two motor – propeller assemblies. The second degree of freedom is the rotation around the pitch axis which is controlled by the difference in the lift forces created by two motor – propeller assemblies. The third and last degree of freedom is the rotation around the travel axis which is controlled by the rate of pitching of the helicopter body.

There are two methods of obtaining an approximate mathematical modeling of the motor – propeller dynamics. First method is by approximating a simple DC motor model to our system. Second method which is more effective and typically produces better results is through testing.

3.1.1 Typical DC motor modeling

The transfer function of the DC motor could be derived by analyzing the figure below,

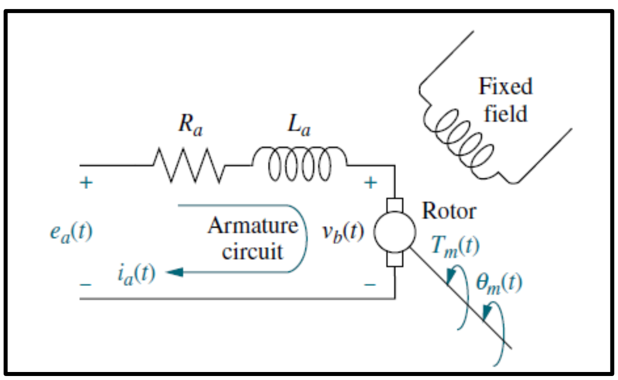

Figure 3.1: DC Motor Schematic [3]

First considering the electrical side of the DC motor

$$R_a I_a(s) + L_a s I_a(s) + V_b(s) = E_a(s) \tag{1}$$

Second by considering the mechanical point of view of the DC motor

$$T_m(s) = K_t I_a(s) \tag{2}$$

By combining both equation (1) and (2) using some algebraic manipulations, ignoring the armature inductance and accounting for the propeller, the following transfer function was obtained,

$$\frac{F}{V} = \frac{k_{mt}.F_w}{(R_m.J_{pm})s + (K_{pt}.R_m + k_{mt}k_b)}$$

As noticed from the above transfer function the motor – propeller dynamics was approximated as a first-order system which could be used in the next section to acquire a model via testing.

The values of K_{mt}, F_w and K_{pt} could only be determined experimentally as shown in Appendix.

Substituting the values of all the constants in the transfer function above yields the following first approximate model,

$$\frac{F}{V} = \frac{1.444}{s + 8.638}$$

3.1.2 Modeling via Testing

Since we have determined from the previous sections that the motor – propeller dynamics could be approximated as first-order system. The following method was conducted to extract a first-order model via testing.

By considering the first-order system diagram shown below,

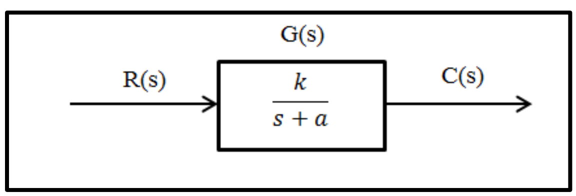

Figure 3.2: First-Order System [3]

A first-order system given by, G(s) = k / (s + a), and a unit step input given by, R(s) = 1 / s. The system response due to a unit step input could be described as following,

$$C(s) = R(s)G(s) = \frac{k}{s(s+a)} = \frac{k/a}{s} - \frac{k/a}{(s+a)}$$

Taking the inverse Laplace transform of the equation,

$$c(t) = \frac{k}{a} - \frac{k}{a}e^{-at}$$

The system response shown above is divided into two parts, first is the forced response term that is originally generated by the step input. Second part of the response is the natural response generated by the system itself.

By comparing the step response generated by the system experimentally to the above first-order system response we could easily construct a first-order model as shown in Appendix.

The results of all the constants determined experimentally were summarized in the table below and the average was taken to approach the final experimental model shown in Equation (3).

Table 3.1: Experimental Results Summarized

	Steady State	k	a
Test 1	2.75	0.43648	2.857
Test 2	2.7	0.34883	2.3255
Test 3	2.7	0.375	2.5608
Average	2.7	0.3868	2.58

$$G(s) = \frac{F}{V} = \frac{0.3868}{s + 2.58} \tag{3}$$

3.1.3 Models Results and Comparison

A simulation was conducted in Matlab to justify the validity of the models constructed above and to provide a viable comparison tool for the performance between the models. The following plot in Figure (3.3) shows an 18 volts step response of the actual test as well as the two models created above.

As shown in the figure below that the step response of the second model constructed (modeling via testing) is a better approximation to the actual system response than the first model which is an adjusted version of the typical DC motor model.

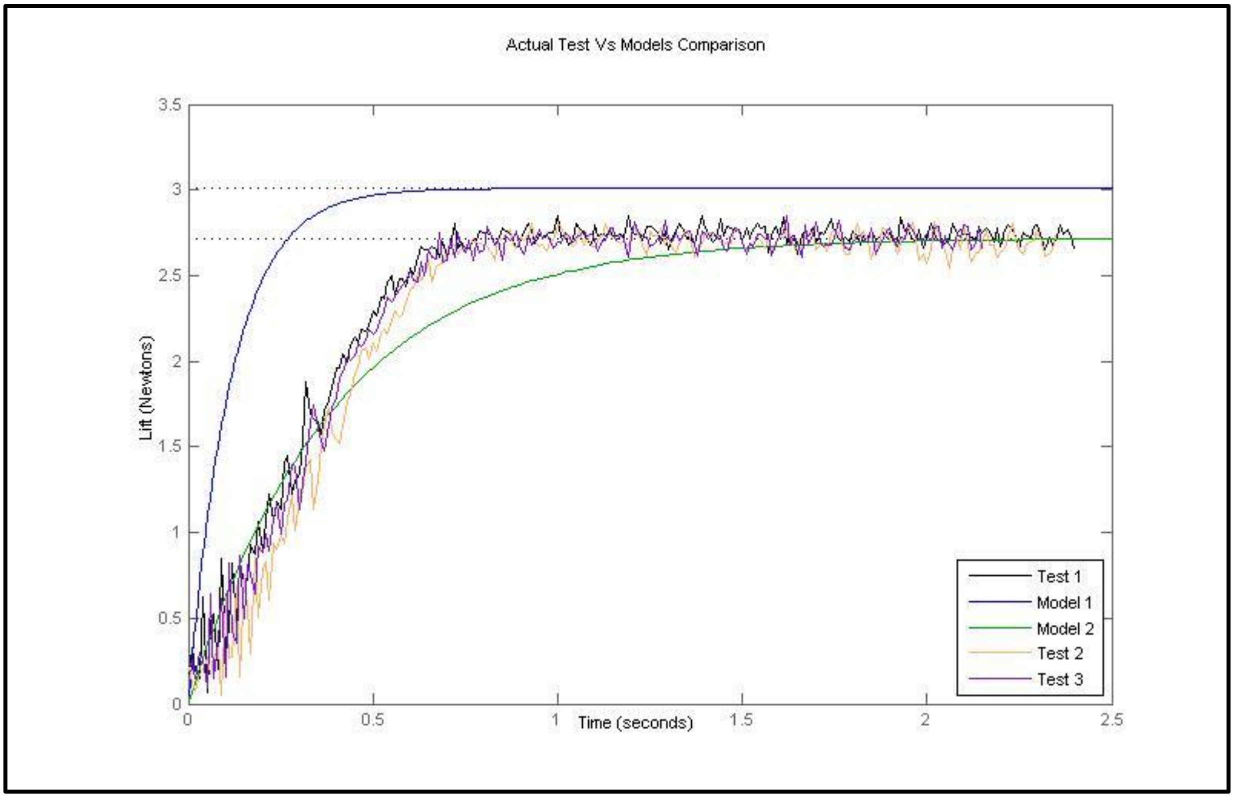

Figure 3.3 : Actual Tests vs Models Comparison

3.2 Pitch Angle Modeling and Simulation

The rotation of the helicopter body around the pitch axis is due to the difference in the lift force created by both motor – propeller assembly units. As shown in the front view diagram of the helicopter in Figure (3.4) the net force acting on the helicopter body could be projected into two forces, F_{sum} and F_{diff}. F_{sum} is the upward lift force which is responsible for the rotation of the helicopter around the elevation axis. F_{diff} is the horizontal force responsible for the rotation of the helicopter around the pitch axis. The rotation around the pitch axis could be modeled analytically as well as it could be derived experimentally by conducting some tests.

3.2.1 Pitch Only Dynamics

The first step of deriving the model rotation of the helicopter body around the pitch axis is by drawing a free body diagram for the helicopter body as shown in Figure (3.5) to analyze the forces acting on it. For the helicopter body to pitch there should be a difference between the lift forces created by both motor – propeller assemblies. As shown in the diagram the lift force of created by the front motor is larger in magnitude than the lift force created by the back motor. The difference between the two lift forces is called F_{diff} which is the force responsible for creating the torque that rotates the helicopter body around its pitch axis.

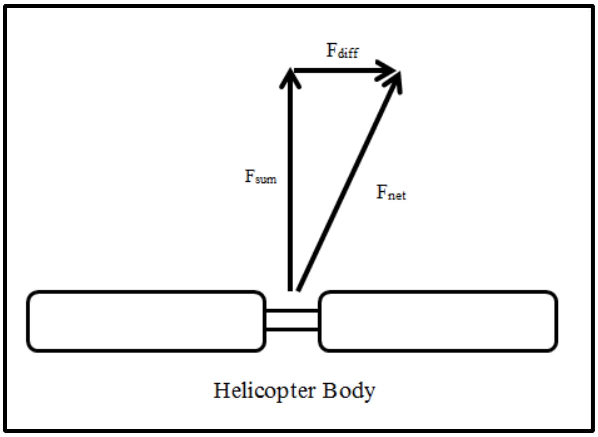

Figure 3.4: : Helicopter Body Equivalent Free Body Diagram

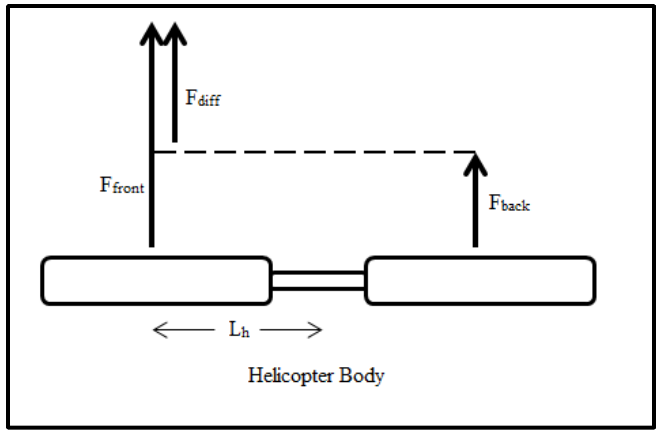

Figure 3.5: : Helicopter Body Actual Free Body Diagram

The following equation could be derived from the diagram above,

$$\left(J_p . s^2 + D_p . s + K_p\right) . \rho(s) = F_{diff} . L_h$$

Since the gravitational force acts on the helicopter body as a restoring force it is adequate to add a restoring torsional constant K_p along the pitch axis.

Then the transfer function of the pitch dynamics could be written as following,

$$\frac{\rho}{F_{diff}} = \frac{L_h}{J_p . s^2 + D_p . s + K_p}$$

D_p the pitch rotation damping force could only be evaluated experimentally as presented in the following section.

3.2.2 Modeling via Testing

Several experimental tests were conducted and the results were obtained to be used to extract the pitch rotation damping coefficient. The helicopter was prepared for testing the pitch rotation by constraining the rotation of the helicopter around the elevation axis and around the travel axis as well. Multiple tests were performed by applying different values of V_{diff} which is the voltage responsible for creating F_{diff} that creates the rotating torque around the pitch axis and measuring the output pitch angle of the helicopter body with respect to time.

The results obtained from the pitch testing was expected to behave as a third order model since the pitch rotation behavior is a combination of both the motor –propeller assembly dynamics which was modeled as a first order system and the pitch only dynamics that was derived as a second order system in the previous section. Since it is difficult to extract any information from a third order model system response, we adopted the assumption of approximating this third order system to a second order system. This approximation would not only allow the extraction of the pitch damping coefficient but also it would be proved later that this approximation is perfectly viable.

Since the pitch rotation responses determined experimentally was approximated to be a second order system, it is then acceptable to use the second order system equations as shown below.

$$\rho = \frac{-\ln(\%OS/100\,)}{\sqrt{\pi^2 + \, ln^2(\%OS/100)}}$$

The equation above describes the damping coefficient as a function of the percentage overshoot; this means that by extracting the percentage overshoot from the experimental responses the damping coefficient could be easily calculated.

The following figure is a sample graph response obtained from the pitch rotation experiments.

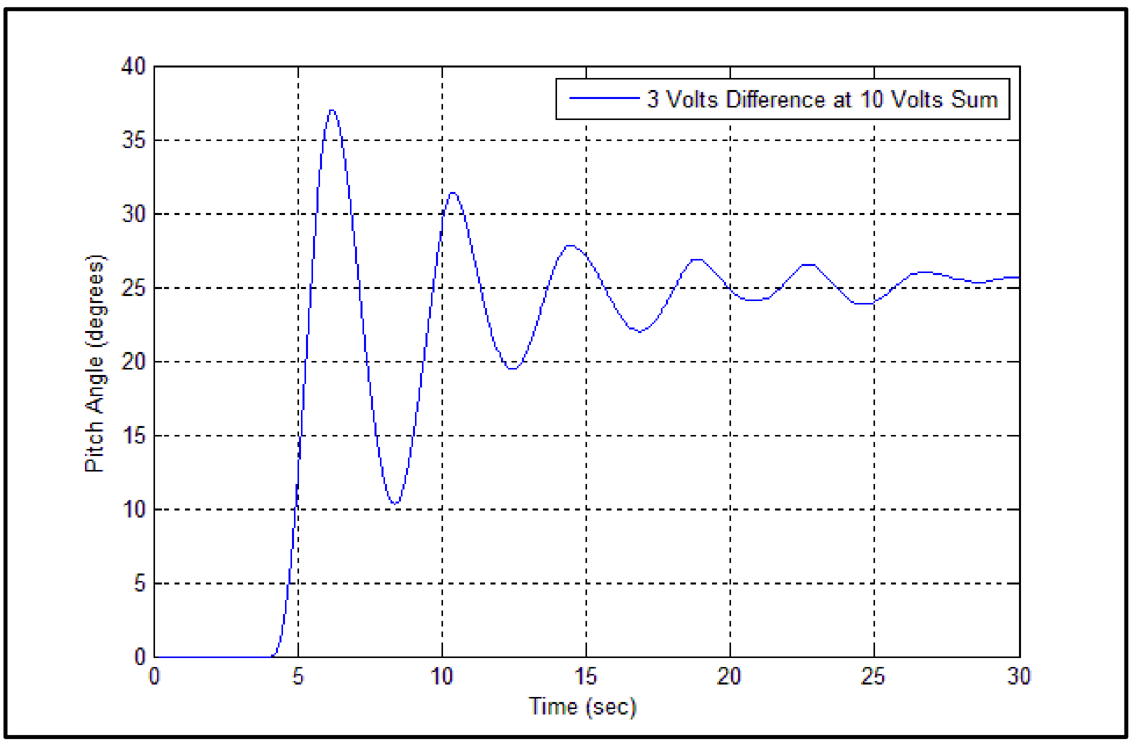

Figure 3.4: 3 Volts Difference Output Response

The experimental results were summarized and presented in the table below and the pitch rotation damping coefficient was approximately calculated to be 0.12.

Table 3.2: Experimental Results Summerized

	Voltage (V)	ω_n	% OS	ρ	K
Test 1	2	1.43	78.1	0.07843	0.2713
Test 2	2.3	1.4	77.42	0.081178	0.291784
Test 3	3	1.52	56	0.182	0.3195
Average		1.45	70.50	0.12	0.295

Using the pitch damping coefficient from the model above we could easily calculate the damping coefficient D_p for the analytical model derived in the previous section using the following simple relation.

$$\frac{D_p}{J_p} = 2 \times \rho \times \omega_n$$

$$D_p = 0.04 \times 2 \times 0.12 \times 1.35 = \mathbf{0.01296}\ \boldsymbol{N.m/rad\,/sec}$$

Then by plugging all the values in the pitch only dynamics model, the following transfer function was obtained.

$$\frac{\rho}{F_{diff}} = \frac{0.178}{0.04s^2 + 0.01296s + 0.1011}$$

3.2.3 Models Results and Simulation

The total pitch rotation dynamics is the combination of both the motor – propeller assembly dynamics and the pitch only dynamics as shown in the figure below,

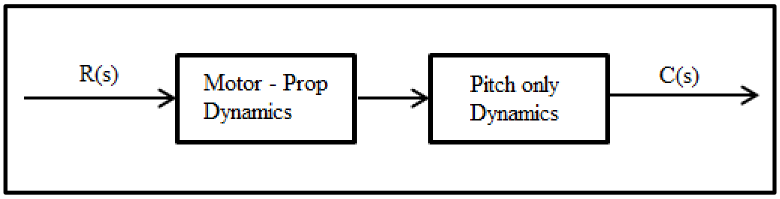

Figure 3.5: Total Pitch Model Block Diagram

By cascading the motor – prop dynamics with the pitch only dynamics and slightly tweaking the gain value from 1.76 to 0.989, the following transfer function for the pitch dynamics was obtained and the model step response result was compared to the actual test in Figure (3.8).

$$\frac{\rho}{V} = \frac{0.035}{0.04s^3 + 0.1154s^2 + 0.1343s + 0.2588}$$

The total pitch dynamics was modeled as shown above as a third order system, which would make the design of the pitch controller a little problematic. The model would be analyzed and checked thoroughly for the possibility of approximating it to a second order model.

The model above is a third order model that has three poles; two are complex poles while the third is located on the negative real axis. The third order model could be approximated to a second order model if the third real pole is far enough to the left on the real axis.

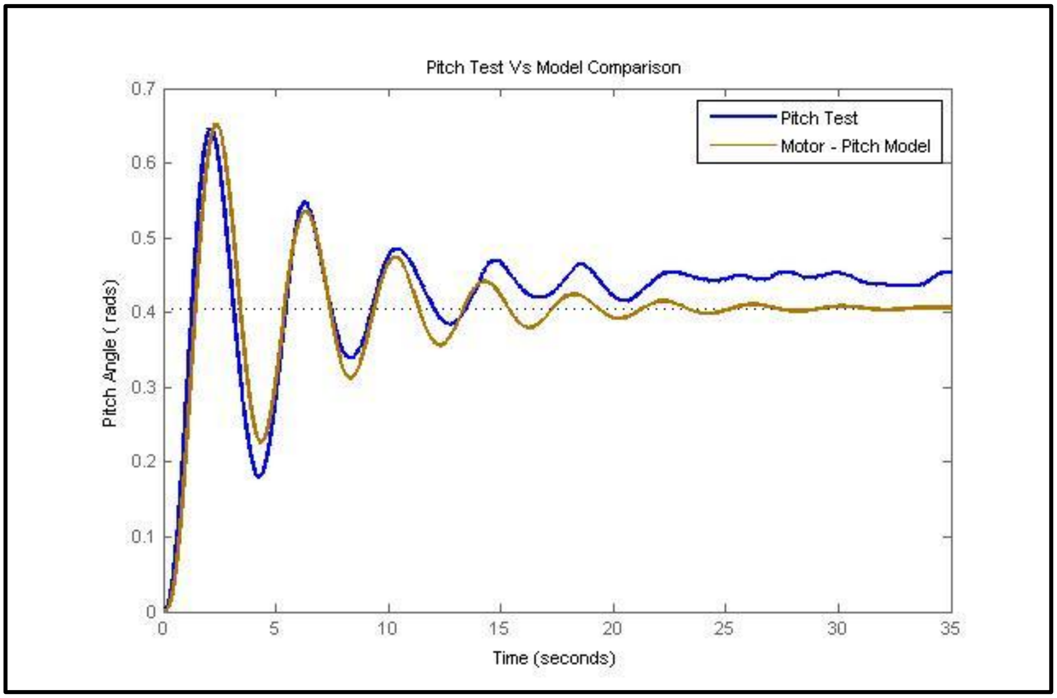

Figure 3.6: Actual Test vs. Model Comparison

The root locus diagram for the pitch model was plotted and shown in Figure (3.9) below. The poles positions were checked and were found to be located at -0.162±1.58j and -2.56. The ratio between the real pole position and the complex poles were calculated and found to be 15.8. For the approximation to be correct the ratio has to be at least 5 times. So we can deduce that the approximation of this model to a second order model is perfectly valid. The pitch model could only be represented by the two complex poles as shown in the transfer function below.

$$\frac{\rho}{V} = \frac{0.35}{s^2 + 0.324s + 2.523}$$

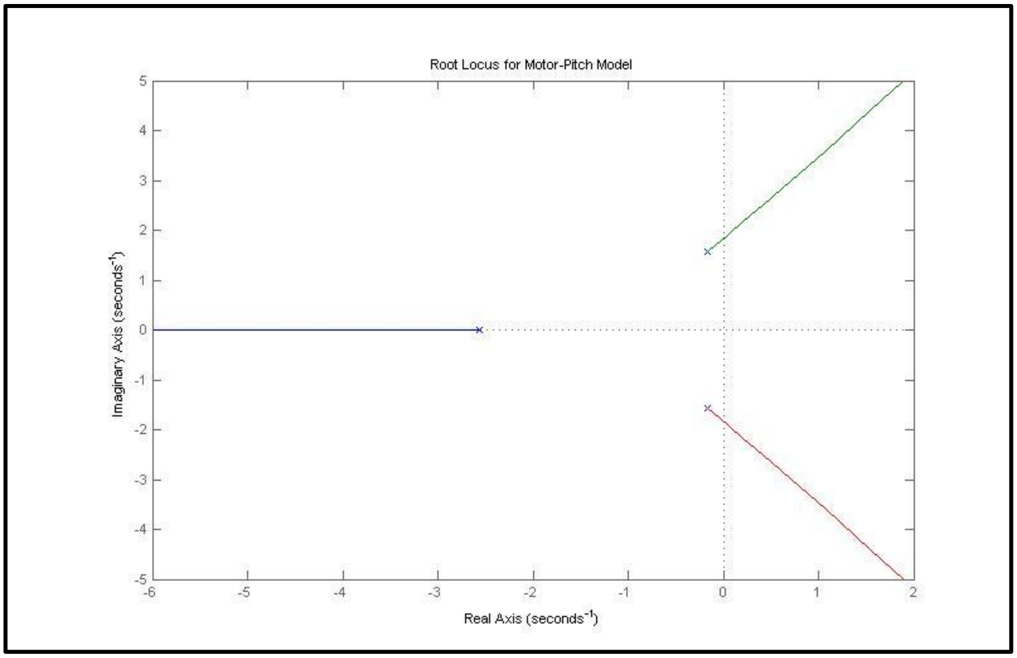

Figure 3.7: Pitch Model Root Locus Diagram

3.3 Travel Angle Modeling

The rotation of the helicopter around the travel axis is a function of the rotation of the helicopter body around the pitch axis. The rate of travel depends on the change rate of the pitch angle of the helicopter body. The dynamics of the helicopter rotation around the travel axis is unlike the motor – propeller dynamics and the dynamics of the rotation of the helicopter body around the pitch axis, it could only be modeled analytically. There is no specific experimental method for modeling the helicopter rotation around the travel axis.

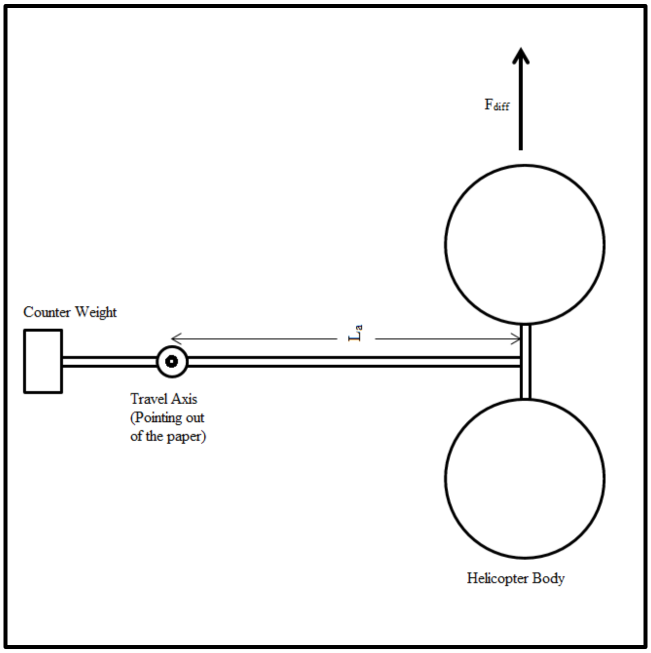

Figure 3.8: Top View of the Helicopter Free Body Diagram.

The first step of modeling the rotation of the helicopter around the travel axis is drawing a free body diagram around the travel axis (plan view of the helicopter) as shown in the Figure (3.10). For simplifying the model we can assume that helicopter is in a constant horizontal position around the elevation axis.

From the diagram above the equation of motion of the helicopter could be written as following,

$$(J_t . s^2 + D_t . s) . \lambda(s) = F_{diff} . L_a$$

Since the rotation of the helicopter around the travel axis depends on the rotation of the helicopter body around the pitch axis, then we could adjust the transfer function of the travel to be a function of the pitch angle as following,

$$\frac{\lambda}{\rho} = \frac{-k_{eff} . L_a}{J_t . s^2 + D_t . s}$$

D_t is the damping coefficient in the travel axis which mainly due to the friction in the travel joint, it could be ignored since it is a really small value. The negative sign in the travel transfer function is due to the fact that the helicopter travels in the negative travel direction when the pitch is positive.

Substituting with the constants values in the equation above yield a travel transfer function model as following,

$$\frac{\lambda}{\rho} = \frac{-0.970794}{1.1726 . s^2}$$

CHAPTER 4: CONTROL DESIGN AND SIMULATION

The purpose of this lab is designing a full travel controller, simulating and evaluating its performance. The Quanser helicopter has three degrees of freedom output and two inputs. The outputs are the rotation around the elevation axis, the pitch axis and the travel axis while the inputs are the two motor – propeller assemblies. The output lift forces of the two motor – propeller assemblies are divided into two vectors; first, F_{sum} that controls the rotation around the elevation axis, second, F_{diff} which controls the rotation around the pitch axis which in turn controls the rotation around the travel axis. For the purpose of this lab, the rotation around the elevation axis would be ignored and assumed constant in a leveled position.

There are different controller designs and configurations such as the cascade compensation controllers and the feedback compensation controllers shown in the figure below. The chosen controller type in this report is the cascade compensation controller. In this configuration the compensator is placed in the forward path in cascade with the plant.

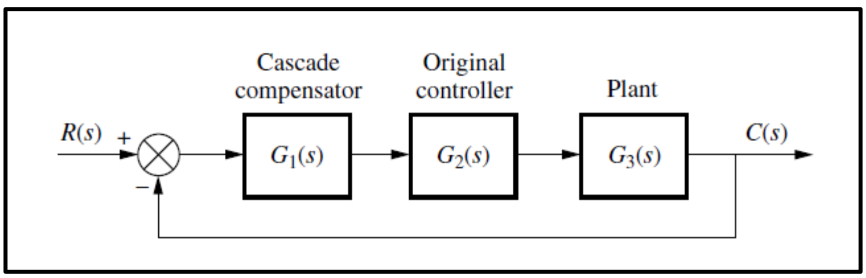

Figure 4.1: Cascade Compensation Configuration [3]

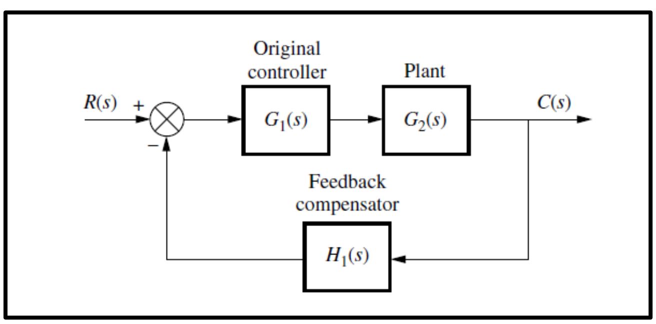

Figure 4.2: Feedback Compensator Configuration [3]

There are different controller types that could be used to improve the system performance such as a PD, PI and PID controllers. There are other types of passive controllers such as lead, lag and lag-lead controllers. Since PID controllers are the most common and are widely used all over the world, it is chosen to be used in pitch and travel control.

4.1 Pitch Control Design

The first step of designing a full travel controller is designing a good pitch controller since the rotation around the pitch axis controls the rotation of the travel axis. The main step of designing a controller would be deciding the design requirements needed and the restrictions and limitations of the system itself. So, we start be evaluating the performance Figure (4.3) of the uncompensated system which would enable us to determine good design requirements.

Table 4.1: Uncompensated System Parameters

Parameters	Values
T_p	1.85 sec
T_s	22.8 sec
% OS	74 %
T_r	0.663 sec

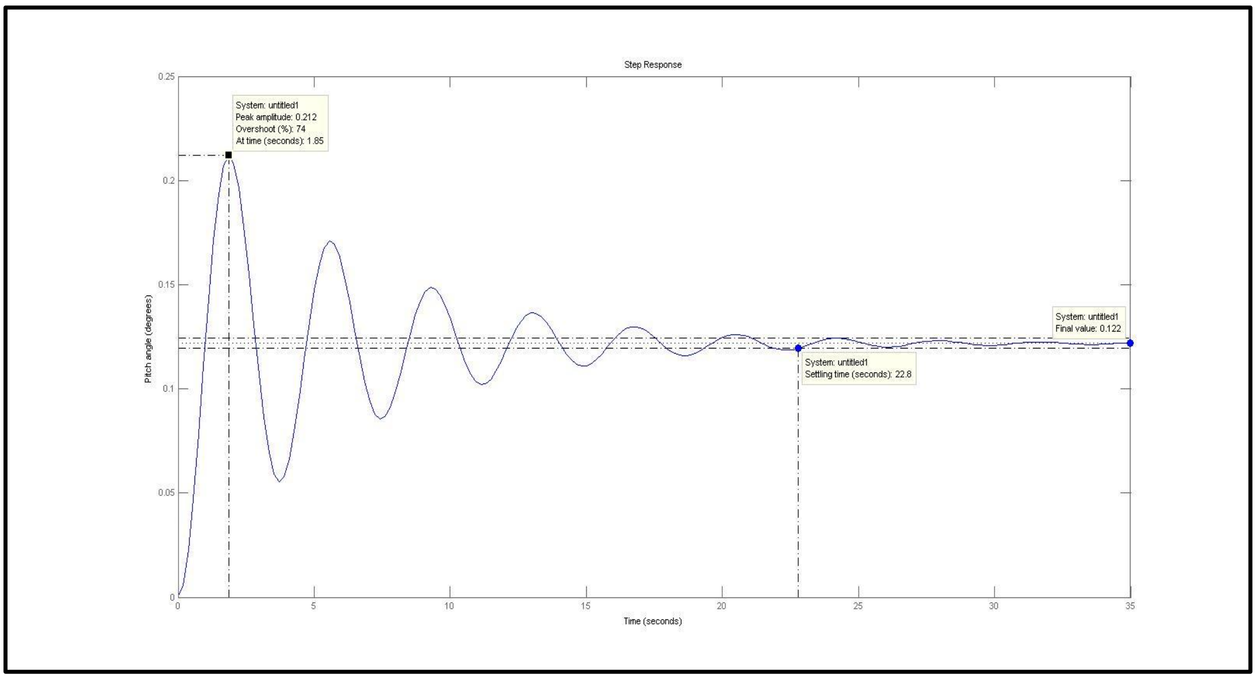

Figure 4.3: Uncompensated System Step response

Design requirements:

1. The response time of the pitch has to be fast enough to control the rotation around the travel axis. The peak time would have to be reduced to half of the value of the uncompensated system.
2. The steady state error of the pitch angle has to be significantly reduced.
3. The %OS would preferably be reduced even though it would not affect the system significantly.
4. The plant input (Pitch dynamics) has to be restricted between -3.5 to 3.5 volts. These are the voltages for reaching a maximum pitch angles.

Design method:

Multiple attempts were conducted to design a PID controller using root locus method. Although the simulations for the responses proved significant improvements as shown below in the sample design, the whole design was ignored for the following reasons:

1. First the PID design could not be simulated using Matlab/Simulink because it couldn't simulate a typical PID controller as it adds a filter in the derivative path of the controller which acts as an extra pole that completely changes the response.
2. Designing a typical PID controller doesn't take into consideration the limitations of the controller outputs.

The following is a sample of a typical PID design which was performed and tested using normal Matlab functions and sisotool.

Table 4.2: Sample PID Design vis Root Locus

Parameters	Values
K_P	67.07393
K_D	2.53916
K_I	6.682
T_p	0.556 sec
T_s	17.5 sec
% OS	55 %
T_r	0.23 sec
$e(\infty)$	0

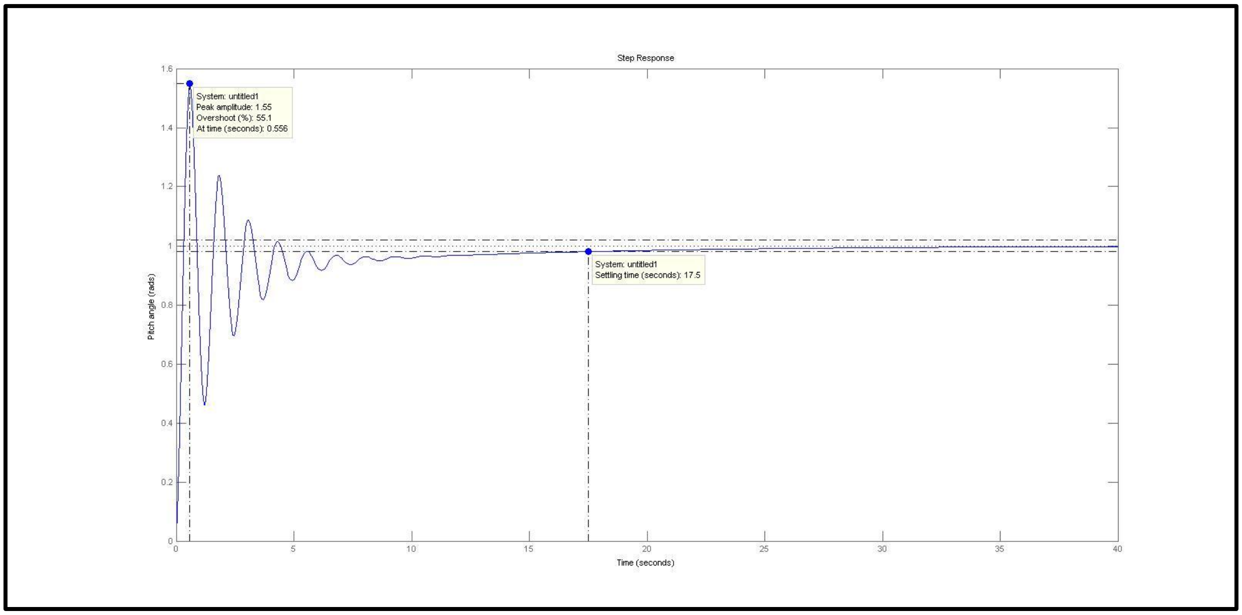

Figure 4.4: Sample System Step Response with Root Locus PID Design

The second method used is Simulink automatic PID tuning which has the following advantages,

1. Allows the restriction of the controller output.
2. Has certain function such as anti-windup method using back calculation that prevents the windup from the integrator path.
3. Allows the user to control the response time for more realistic designs.

Table 4.3: Simulink Pitch PID Tuned Parameters

Parameters	values
K_P	24.6471
K_D	10.9125
K_I	6.5035
N	26.515
kb	0.07
T_s	11.7 sec
T_p	0.592 sec
$e(\infty)$	0

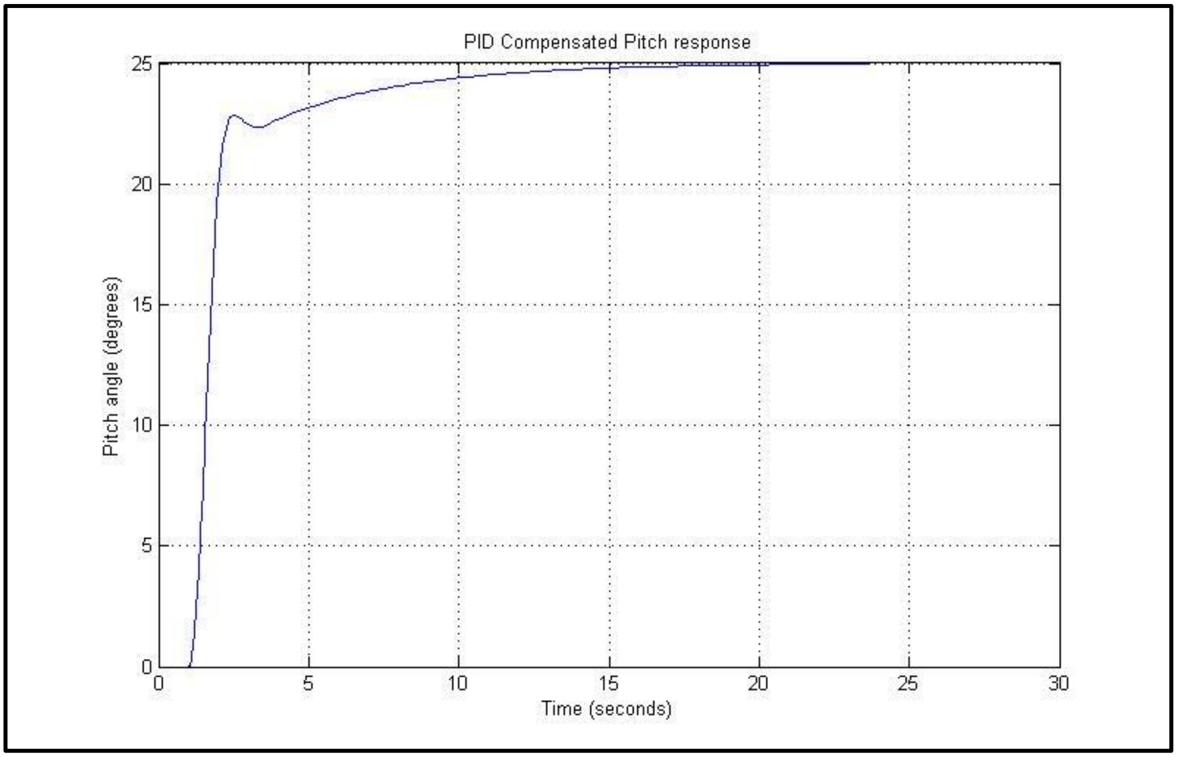

Figure 4.5: Pitch Step response with Simulink PID Design

4.2 Travel Control Design

The pitch control was an essential element in designing the travel controller since a good travel control mainly depends on the effectiveness of the pitch controller. The travel controller would also be a cascade compensation design and a PID controller as well. The figure below shows the schematic block diagram for the travel controller.

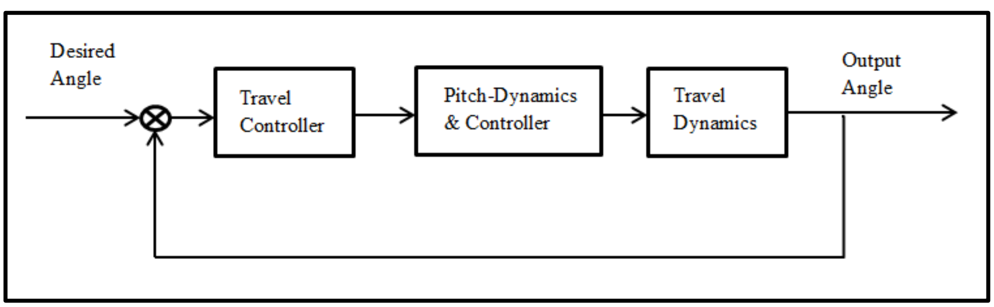

Figure 4.6: Travel Controller Block Diagram

The output of the travel controller should be restricted between -25 to 25 degrees as it is the input for the pitch controller. Using Simulink PID designing tool for the reasons mentioned in the section above the following controller parameters were obtained,

Table 4.4: Simulink Travel PID Tuned Parameters

Parameters	Values
K_P	-0.007212
K_D	-0.4588
K_I	-1.6e-04
N	0.8285
kb	0.07
T_s	55 sec
T_p	11 sec
e(∞)	0

The following figure shows the response of the travel – pitch controller for a 40 degrees desired angle input. As noted the time needed for the peak response is approximately 11 seconds. It was also noted that the settling time needed was about 55 seconds. The controller was tested for different desired input angles and it was found that the maximum input angle for operating within the given performance parameters is approximately 45 degrees. The controller doesn't respond to higher angle inputs as expected.

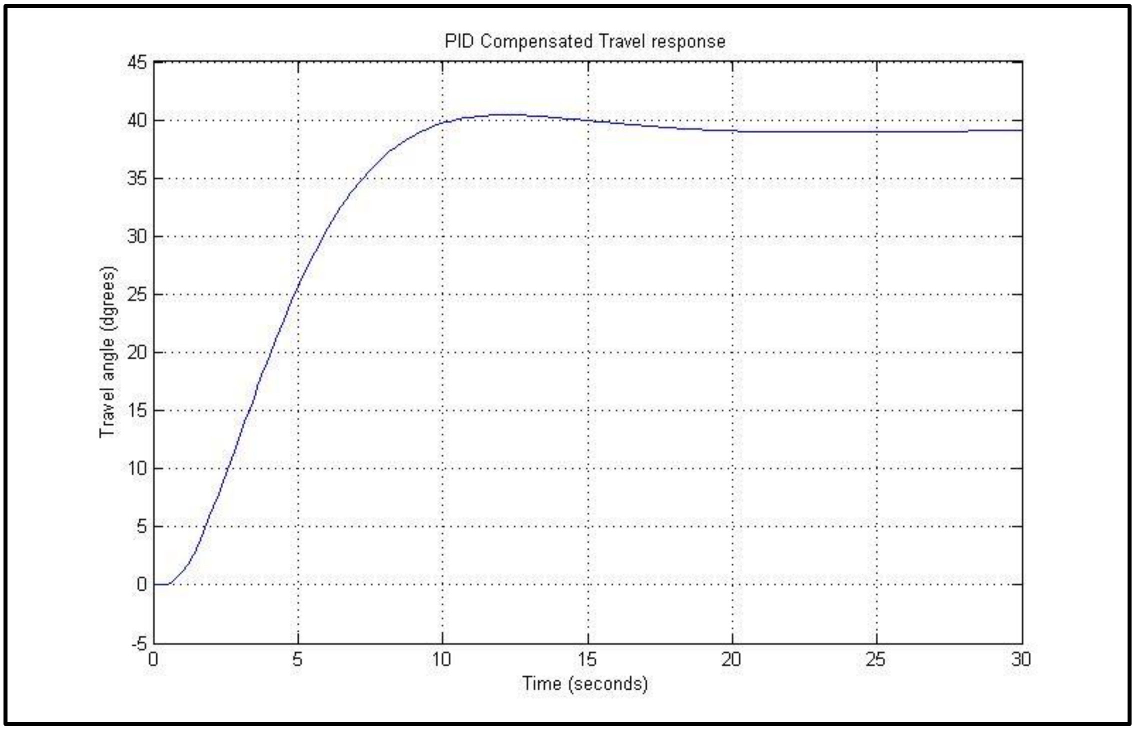

Figure 4.7: Travel Step response with Simulink PID Design

CHAPTER 5: SUMMARY AND CONCLUSION

In this report, the helicopter motor- propeller dynamics, pitch dynamics and travel dynamics were modeled separately and combined together. Simulations were used to prove the validity of all the models created for the helicopter. Multiple attempts were performed to design pitch and travel PID controllers using cascade compensation configuration. The typical known method for designing a PID controller using root locus diagram had its own disadvantages which lead to the rejection of all the controllers designed analytically. Multiple attempts were also performed to design lag-lead compensators and using Matlab/sisotool/optimization tool to reach a better system performance. These attempts yielded unsuccessful system output responses which led to the use of Matlab/Simulink PID automatic tuning tool. The results presented in this report were the best system responses outputs that was achieved so far. The travel controller responses demonstrated poor overall system performance. Future work would include a better analytical systematic approach for designing a travel – pitch controllers, tackling all the problems emerged from having limitation on the controllers' outputs and simulating a typical PID controller and finally improving the design requirements and system performances.

REFERENCES

[1] Enright, J., & Cresnik, P. (Winter 2013). *Updated and Extended Information.* Ryerson.

[2] Golnaraghi, F., & Kuo, B. (2010). *Automatic Control Systems.* John Wiley.

[3] Nise, N. (2004). *Control Systems Engineering.* John Wiley.

[4] Quanser 3-DOF Helicopter Reference Manual. (n.d.).

APPENDIX

- *Determining DC Motor Model Constants*

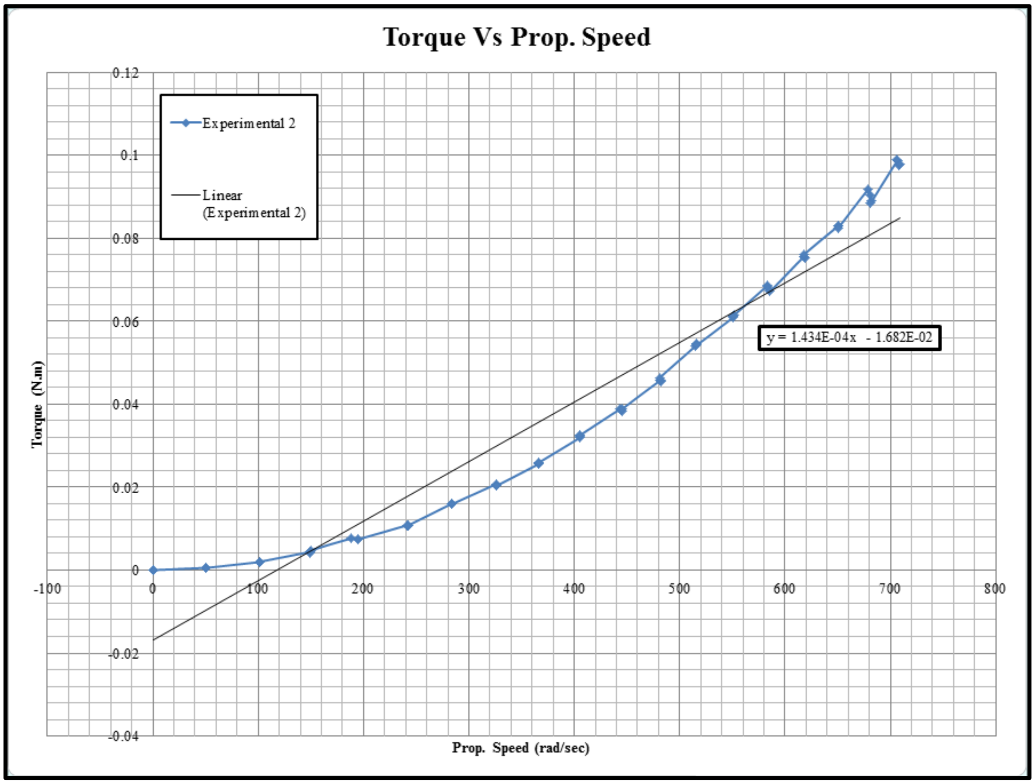

Figure A.1: Troque vs Prop. Speed

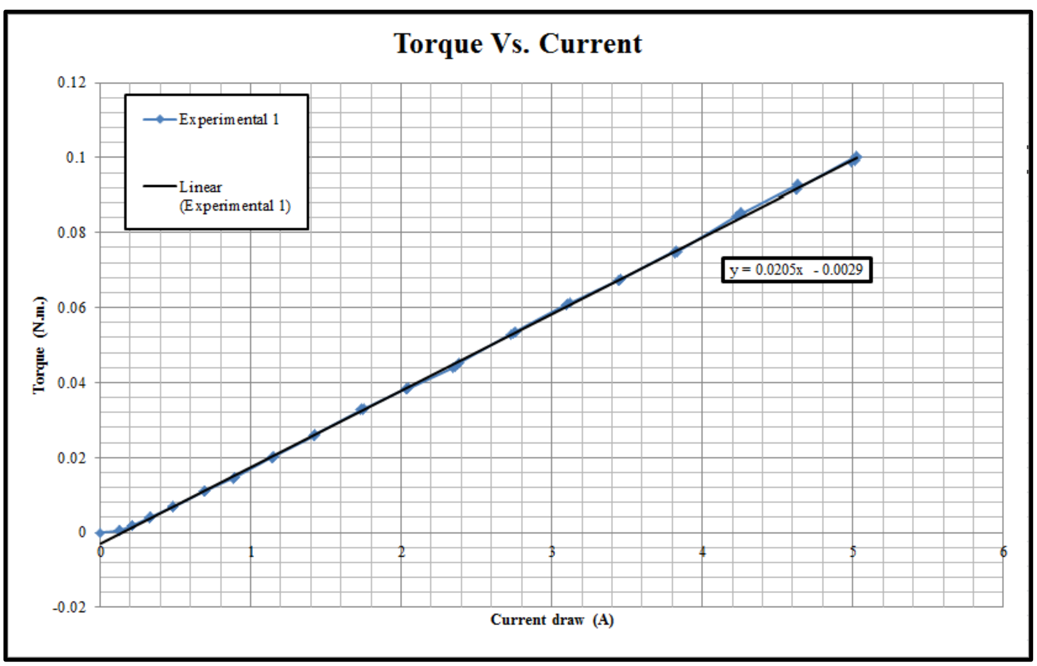

Figure A.2: Torque vs Current

- *Experimental DC motor model*

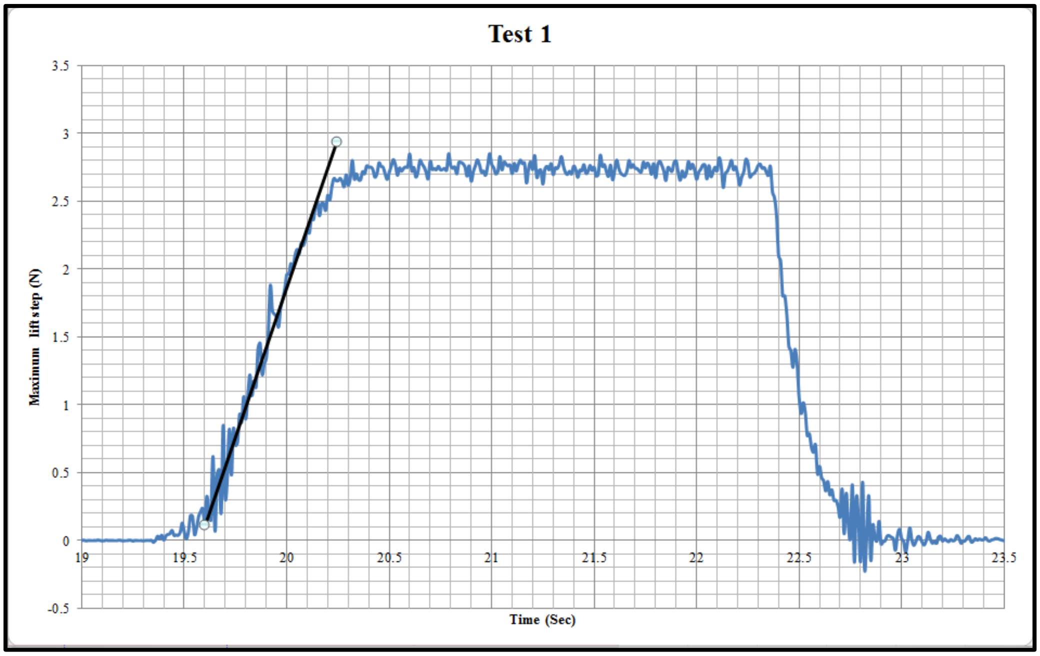

Figure A.3: Motor - Prop Test 1

- *Simulink diagrams*

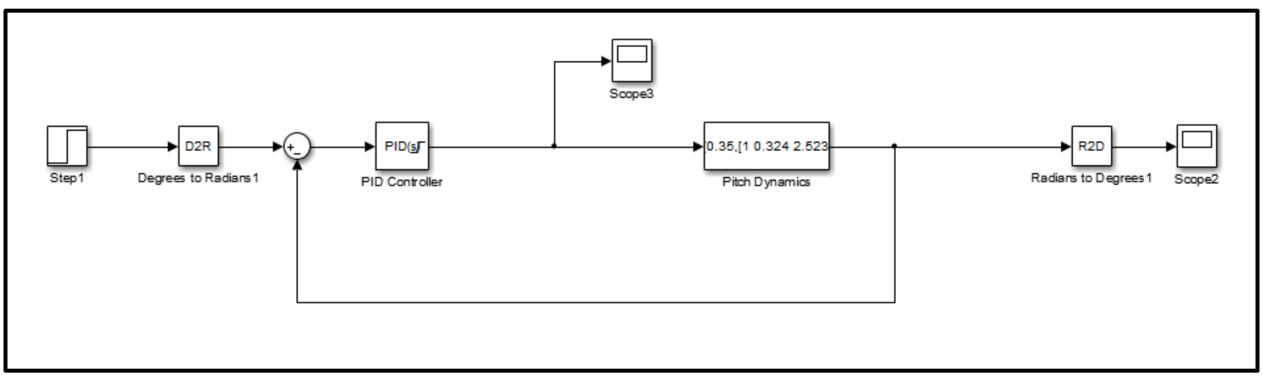

Figure A.4: Simulink Pitch Controller Block Diagram

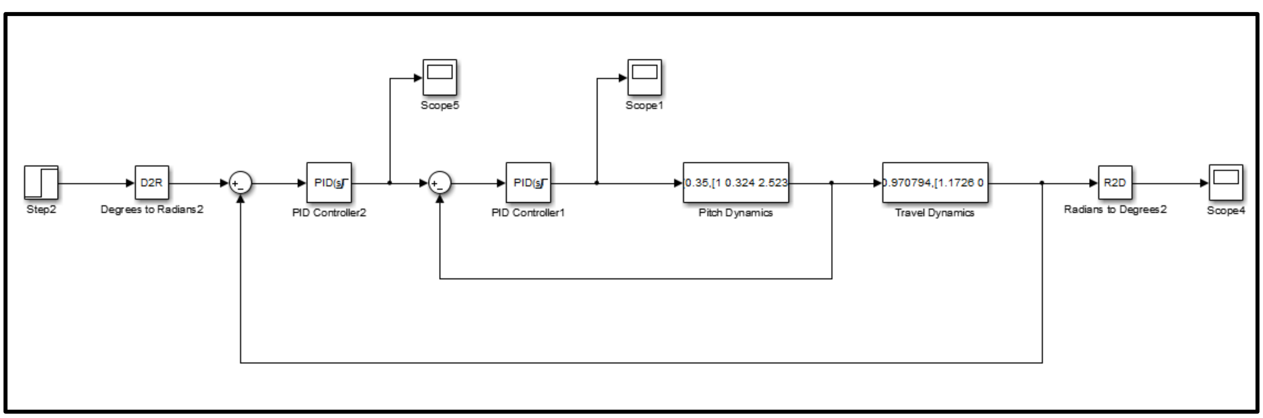

Figure A.5: Simulink Travel Controller Block Diagram